Effective Use of Molecular Recognition in Gas Sensing: Results from Acoustic Wave and in Situ FT−IR Measurements

ARTICLE *in* ANALYTICAL CHEMISTRY · SEPTEMBER 1999

Impact Factor: 5.64 · DOI: 10.1021/ac981311j · Source: PubMed

4 AUTHORS, INCLUDING:

Andreas Hierlemann
ETH Zurich
290 PUBLICATIONS **4,834** CITATIONS
SEE PROFILE

Antonio Ricco
Stanford University
248 PUBLICATIONS **4,644** CITATIONS
SEE PROFILE

Effective Use of Molecular Recognition in Gas Sensing: Results from Acoustic Wave and in Situ FT-IR Measurements

Andreas Hierlemann,*,†,‡ Antonio J. Ricco,*,†,§ Karl Bodenhöfer,|| and Wolfgang Göpel||

Microsensor Research & Development Department, Sandia National Laboratories, Albuquerque, New Mexico 87185-1425, and Institut für Physikalische und Theoretische Chemie, Universität Tübingen, Auf der Morgenstelle 8, 72076 Tübingen, Germany

To probe directly the analyte/film interactions that characterize molecular recognition in gas sensors, we recorded changes to the in situ surface vibrational spectra of specifically functionalized surface acoustic wave (SAW) devices concurrently with analyte exposure and SAW measurement of the extent of sorption. Fourier transform infrared external-reflectance spectra (FT-IR-ERS) were collected from operating 97-MHz SAW delay lines during exposure to a range of analytes as they interacted with thin-film coatings previously shown to be selective: cyclodextrins for chiral recognition, nickel camphorates for Lewis bases such as pyridine or organophosphonates, and phthalocyanines for aromatic compounds. In most cases where specific chemical interactions—metal coordination, "cage" compound inclusion, or π-stacking—were expected, analyte dosing caused distinctive changes in the IR spectra, together with anomalously large SAW sensor responses. In contrast, control experiments involving the physisorption of the same analytes by conventional organic polymers did not cause similar changes in the IR spectra, and the SAW responses were smaller. For a given conventional polymer, the partition coefficients (or SAW sensor signals) roughly followed the analyte fraction of saturation vapor pressure. These SAW/FT-IR results support earlier conclusions derived from thickness-shear mode resonator data.

High chemical selectivity and rapid reversibility can place contradictory constraints on desired interactions between chemical sensor coating materials and analytes. Low-energy, perfectly reversible (physisorptive) interactions generally lack high selectivity, while chemisorptive processes, the strongest of which result in the formation of new chemical bonds, offer selectivity, but are inherently less reversible. One solution to this problem is to use arrays of sensing materials together with pattern recognition methods;[1−4] another is to discover or develop fully reversible "intermediate" interactions, lying at the weak end of chemisorption (<120 kJ/mol), but exceeding simple physisorption (0−30 kJ/mol). Such systems are often characterized by a spatially organized collection of physical interactions. Sensor coatings capable of such "molecular recognition" can play an important role in devising a selective and reversible system.

In the context of gas-phase chemical sensors, the meaning of molecular recognition, along with methods for its effective application, warrants discussion. Lehn et al. state that molecular recognition "implies a structurally well-defined pattern of intermolecular interactions":[5] two species must complement one another in size, shape, and binding or functionality.[6,7] The maximum level of specificity, as realized in biological systems using lock-and-key interactions, is difficult to duplicate in gas/film interactions, where (1) binding has a significant entropic component (largely independent of both coating and analyte), due to the change of the analyte's phase from gas to solution, and (2) the reversible changes in solvation that accompany, for example, the reorientation of a protein or the coordination of an ion are particularly difficult to realize. Nonetheless, clever design of the overall sensing "scheme" can compensate for these handicaps.

A special case of molecular recognition, the detection of enantiomers, is not possible using conventional, nonchiral polymers. For example, the two enantiomers of several analytes have been differentiated, and even quantified accurately in enantiomeric mixtures, by comparing the responses from a pair of coatings based on the complementary enantiomers of chiral amides.[8] This

† Sandia National Laboratories.

‡ Present address: Physical Electronics Laboratory, IQE, ETH Hoenggerberg HPT-H4.2, CH-8093 Zurich, Switzerland. Phone: ++41-1-633-3494. Fax: 41-1-633-1054. E-mail: hierlema@iqe.phys.ethz.ch.

§ Present address: ACLARA Biosciences, Inc., 1288 Pear Ave., Mountain View, CA, 94043; aricco@aclara.com.

|| Universität Tübingen.

(1) Carey, W. P.; Beebe, K. R.; Kowalski, B. R. *Anal. Chem.* **1986**, *58*, 149−153.

(2) Ballantine, D. S.; Rose, S. L.; Grate, J. W.; Wohltjen, H. *Anal. Chem.* **1986**, *58*, 3058−3066.

(3) Osbourn, G. C.; Bartholomew, J. W.; Ricco, A. J.; Crooks, R. M. *Acc. Chem. Res.* **1998**, *31*, 297. Ricco, A. J.; Crooks, R. M.; Osbourn, G. C. *Acc. Chem. Res.* **1998**, *31*, 289.

(4) Hierlemann, A.; Schweizer-Berberich, M.; Weimar, U.; Kraus, G.; Pfau, A.; Göpel, W. Pattern Recognition and Multicomponent Analysis. In *Sensors Update*; Baltes, H., Göpel, W., Hesse, J., Eds.; VCH: Weinheim, Germany, 1996.

(5) Lehn, J. M. *Angew. Chem., Int. Ed. Engl.* **1988**, *27*, 89−112.

(6) Lehn, J. M. *Science* **1985**, *227*, 849.

(7) Rebek, J. *Science* **1987**, *235*, 1478−1484.

(8) Bodenhöfer, K.; Hierlemann, A.; Seemann, J.; Gauglitz, G.; Christian, B.; Koppenhoefer, B.; Göpel, W. *Nature* **1997**, *387*, 577; *Anal. Chem.* **1997**, *69*, 3058−3068.

10.1021/ac981311j CCC: $18.00
Published on Web 00/00/0000

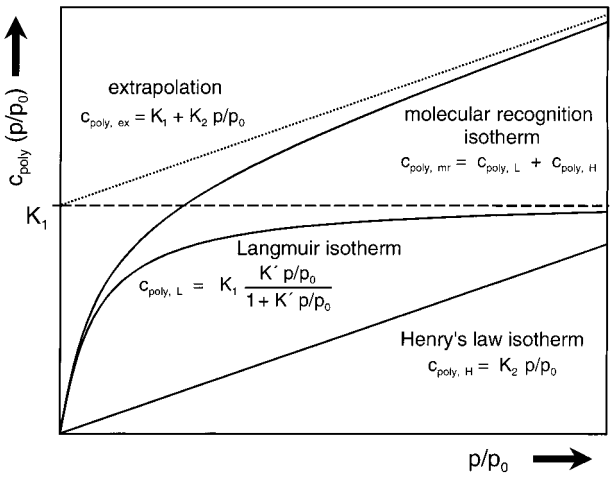

Figure 1. Isotherms representing concentration of analyte sorbed by polymer films for nonspecific (*Henry's law,* $c_{poly,H}$) and chemically specific (*Langmuir,* $c_{poly,L}$) interactions; the isotherm for a "real-world" *molecular recognition* material ($c_{poly,mr}$) sums these contributions. The *extrapolation* yields the number of specific sites in the molecular recognition material. By plotting molar concentration of analyte sorbed in the polymer (c_{poly}) vs fraction of saturation vapor pressure (p/p_0), thermodynamically valid direct comparison of responses from analytes having widely different vapor pressures and molecular weights can be made.

is not a precise embodiment of "perfect recognition using one coating for one analyte", because the sensor responses from the two enantiomeric coatings differ by as little as 10−30%, but the end result is highly effective enantiospecific recognition of a particular compound. Enantiospecific detection has also been demonstrated using supramolecular cages such as cyclodextrins (CDs).[9]

The overall sorption characteristics of molecular recognition materials generally differ fundamentally from those of conventional polymers; this is illustrated in Figure 1.[9] Molecular recognition isotherms exhibit pronounced nonlinearity—basically, Langmuirian behavior in the low concentration range where preferential sorption sites are being filled (similar results are reported, e.g., for paracyclophanes in ref 10). At concentrations where the specific sites are filled, the behavior of a molecular recognition coating resembles that of a conventional polymer: the isotherm is linear up to the concentration at which Henry's law is no longer valid.[8] This occurs for fractional saturation (p/p_0) values as low as 5% or as high as 15%, at which point nonunity activity coefficients must be accounted for. In addition, there is an inevitable additive contribution from nonspecific sorption even at low concentrations, because it is generally impossible to design a film that has only specific sorption sites. The molecular recognition isotherm hence is the sum of a Langmuir and a Henry's law isotherm (Figure 1).

TSMR-measured (TSMR = thickness-shear mode resonator) isotherms for sorption of analytes by a cyclodextrin,[9] the phthalocyanines,[11] and nickel camphorate[12] have been analyzed; they resemble in form the molecular recognition isotherm of Figure 1. Extrapolation and fitting of those isotherms showed that roughly 80% of the calculated number of specific sorption sites are filled for all three materials, suggesting that about 20% of the specific sites are inaccessible in the solid-phase molecular recognition films.

In contrast to molecular recognition materials, nonspecific (conventional) polymers (poly(etherurethane) and poly(isobutene), for example) show a very linear response vs concentration with a zero intercept, consistent with a Henry's law isotherm (Figure 1). This is simple physisorptive behavior.

Equilibrium coefficients for partitioning into molecular recognition films for specifically detected target analytes at low concentrations (usually below 1−2% of p_0) are typically 5−100 times larger than those of nonspecifically recognized analytes (at equivalent p/p_0) or those of the specifically detected analytes sorbed by conventional organic polymers. We note, however, that the presence of a shape-, size-, or functionality-specific interaction does not automatically imply a far stronger interaction than "simple" physisorption. In most cases, inclusion into cage compounds, for example, is a consequence of the "normal" spectrum of physical and very weak chemical interactions: van der Waals, hydrogen bonding, and weak electrostatic or coordination bonds. It is the geometrical arrangement of several to many such interactions in a single host that provides a significantly stronger interaction for certain orientations, shapes, and/or sizes of analyte molecules.

A number of reports attribute shape or class selectivities to cage compounds for sorption of various analytes.[13−16] Some of these "selectivities", however, correlate more strongly with key thermodynamic properties of the analytes (e.g., saturation vapor pressure) than with a demonstrable specific interaction or recognition process. Consequently, the general idea of molecular recognition in gas sensors was questioned by Grate et al.[17] Nonetheless, we recently presented convincing evidence for specific recognition of certain target analytes, including the discrimination of enantiomers using supramolecular cages[9] and the detection of Lewis basic, nitrogen-containing volatile organic compounds (VOCs) using metal coordination;[11] ongoing investigations of phthalocyanines provide further evidence for specific recognition.[12] In this paper, we present detailed molecular spectroscopic evidence to support claims of specific interactions for several coating materials and analytes.

We systematically investigated three coating materials, depicted in Figure 2, previously shown to be selective for gas sensors[9,11,12] and offering three different types of reversible interactions stronger than simple physisorption:

(a) The first type is bucketlike supramolecular compounds, in this case the cyclodextrins. Oriented adsorption of analyte molecules within the CD torus appears to control the recognition process. Since the γ-cyclodextrin derivative used has a large cavity,

(9) Bodenhöfer, K.; Hierlemann, A.; Juza, M.; Schurig, V.; Göpel, W. *Anal. Chem.* **1997**, *69*, 4017−4031.
(10) Dickert, F. L.; Haunschild, A.; Kuschow, V.; Reif, M.; Stathopulos, H. *Anal. Chem.* **1996**, *68*, 1058−1061.
(11) Hierlemann, A.; Bodenhöfer, K.; Fluck, M.; Schurig, V.; Göpel, W. *Anal. Chim. Acta* **1997**, *346*, 327.
(12) Fietzek, C.; Bodenhöfer, K.; Hees, M.; Haisch, P.; Hanack, M.; Göpel, W. *Proc. Eurosensors 1998*, Southhampton, England, manuscript in preparation.
(13) Dickert, F. L.; Bruckdorfer, T.; Feigl, H.; Haunschild, A.; Kuschow, V.; Obermeier, E.; Bulst, W.; Knauer, U.; Mages, G. *Sens. Actuators, B* **1993**, *13−14*, 297−301.
(14) Dickert, F. L.; Haunschild, A. *Adv. Mater.* **1993**, *5*, 887−895.
(15) Schierbaum, K. D.; Weiss, T.; Thoden van Velzen, E. U.; Engbersen, J. R.; Reinhoudt, D. N.; Göpel, W. *Science*, **1994**, *265*, 1413−1415.
(16) Nelli, P.; Dalcanale, E.; Faglia, G.; Sberveglieri, G.; Soncini, P. *Sens. Actuators, B* **1993**, *13−14*, 302−304.
(17) Grate, J. W.; Patrash, S. J.; Abraham, M. *Anal. Chem.* **1996**, *68*, 913.

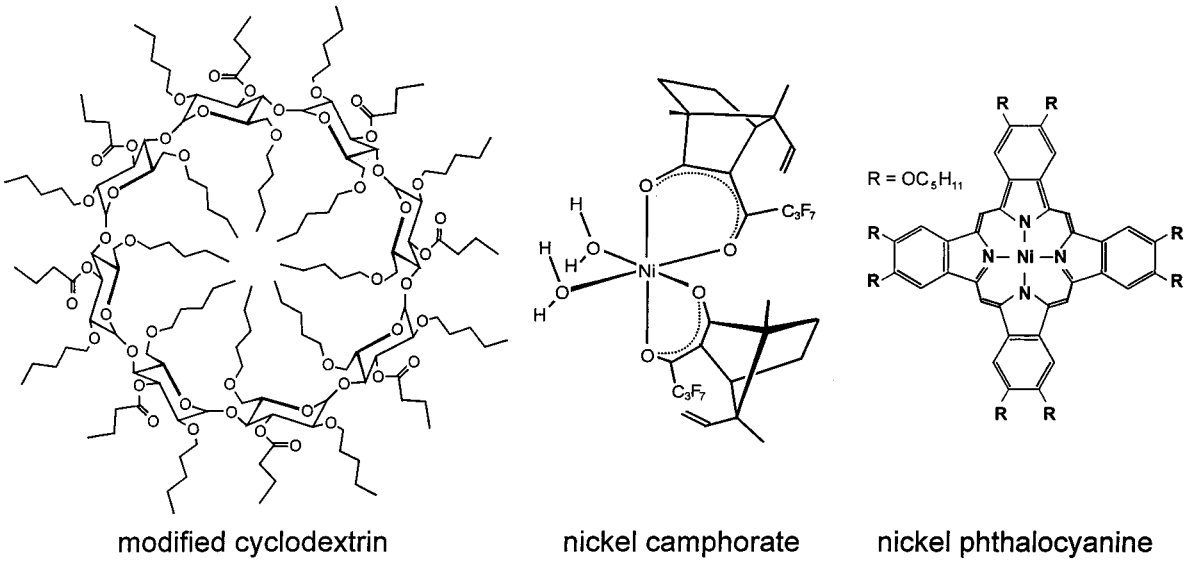

Figure 2. Molecular recognition compounds used in this study.

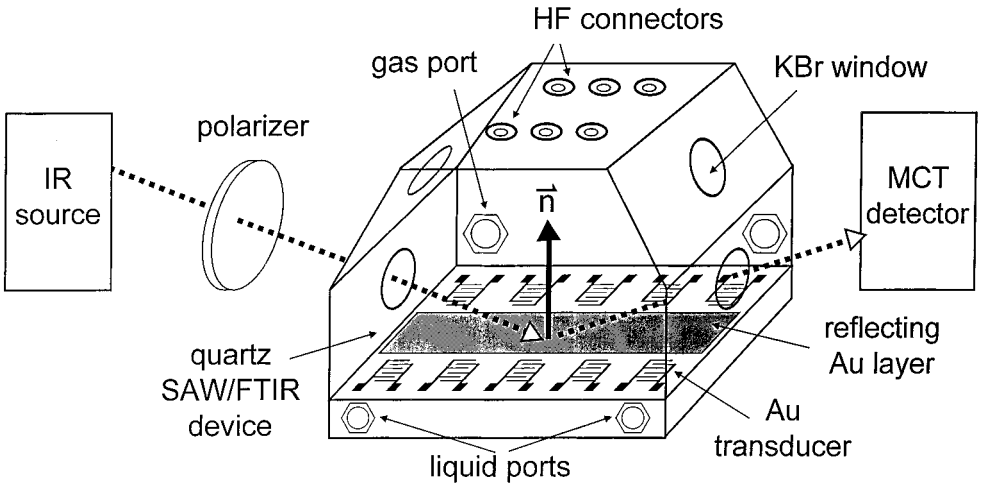

Figure 3. Measurement setup to perform simultaneous SAW/in situ FT-IR external reflectance measurements.

and the torus is not rigid, the determining factor is not simple shape or size selectivity. These cage compounds were used earlier as coatings on TSMRs to demonstrate chiral recognition with gas sensors.[9]

(b) The second type is soluble phthalocyanines (films composed of the pure polycrystalline material). The specific interaction is most likely "π stacking", an intense interaction between the large, delocalized π-electron systems of the phthalocyanines and those of volatile aromatic analytes such as benzene, toluene, and xylene (BTX).[12]

(c) The third type is metal coordination compounds, represented here by nickel camphorates (films composed of the pure polycrystalline material). In the case of nickel camphorate, the specific interaction is probably a coordinative ligand−metal donor bonding of oxygen- or nitrogen-containing analytes to the Ni atom of the chelate complex. The two water molecules shown in Figure 2 are highly labile; previous studies with coordinatively unsaturated Cu^{2+} shows that such ligands can be displaced readily by analytes under conditions of somewhat slow (minutes) but complete reversibility.[11,18]

To understand these specific interactions in more detail, we performed combined SAW/in situ FT-IR-ERS measurements using the experimental setup shown in Figure 3. The film-coated SAW device, the intertransducer region of which acts as a reflector for the IR beam at grazing incidence, is exposed to various VOCs. From simultaneously recorded changes in device frequency (principally due to mass changes) and changes in the IR spectrum of the sorbed VOC, we draw fundamental conclusions about coating/analyte interactions. Appropriate control experiments, using conventional organic polymers expected to exhibit only simple physisorption interactions with the analytes, were conducted to compare and validate the results.

The fundamentals of FT-IR-ERS of organic thin films are described elsewhere.[19−23] Generally, FT-IR-ERS on Au substrates is sensitive to both the polarization state and angle of incidence of the infrared radiation.[24,25] The sum of the incident and image

(18) Thomas, R. C.; Yang, H. C.; DiRubio, C. R.; Ricco, A. J.; Crooks, R. M. *Langmuir* **1996**, *12*, 726.
(19) Greenler, R. G. *J. Chem. Phys.* **1966**, *44*, 310.
(20) Ferraro, J. R.; Basile, L. J. *Fourier transform Infrared Spectroscopy*; Academic Press: New York, 1985; Chapters 7 and 8.
(21) Yates, J. T., Jr.; Madey, T. E. *Vibrational Spectroscopy of Molecules on Surfaces*; Plenum Press: New York, 1987; Chapter 7.
(22) Bubeck, C.; Holtkamp, D. *Adv. Mater.* **1991**, *3*, 32.
(23) Porter, M. D. *Anal. Chem.* **1988**, *60*, 1143A.

(in the surface of the metal) electric vectors for s-polarized radiation produces essentially no electric field at the film/Au interface at all angles of incidence, which prevents IR absorption by any near-surface dipole. In contrast, the vectors of the incident and image electric vectors for p-polarized IR radiation are additive, resulting in an electric field with a nonzero component perpendicular to the surface, with a maximum amplitude measured at near-grazing incidence (for gold, >89.5° from normal).[19−21,24] Thus, surface-confined or near-surface molecules having a dipole component oriented perpendicular to the surface absorb only p-polarized IR radiation (the so-called "surface selection rule").

To enhance the magnitude of the IR absorbance signal, particularly for subtle spectral changes, we applied relatively thick layers of the sensitive coating materials (0.5−1 μm; the surface selection rule applies within approximately one-quarter wavelength of the surface, or 2.5−0.7 μm for the 1000−3500 cm^{-1} range[26]). The films were deposited using spray coating, resulting in grainy or pebbly films with high surface area (speeding absorption), randomly oriented surface features (causing multiple reflection or scattering), and no overall molecular order within the film. Hence, s-polarized IR radiation was absorbed by all the coating materials as well, but with markedly lower absorbance than for the p wave.

For both polarizations, the analyte molecules in the gas phase also absorb IR radiation, contributing to the total signal. Therefore, appropriate background spectra using both polarization states for each coating material and for each gas-phase analyte (at multiple concentrations) were first acquired for reference purposes.

SAW/IR devices consist of five parallel sets of input and output interdigital transducers formed on a large piezoelectric quartz substrate (Figure 3)[27] to accommodate the gold reflection layer. An alternating voltage applied to each input transducer launches a Rayleigh wave that traverses the crystal surface. The output transducer converts the wave back into an electrical signal. Any change in a physical property of the SAW device or a film overlay on the surface that affects either (or both) of the wave propagation parameters, velocity and attenuation, can be exploited to construct a sensor.[28] In addition to mass-loading effects, changes in the velocity and attenuation of the surface acoustic wave can result from changes in the viscoelastic properties of surface-confined layers.[28,29]

To complement results from SAW/FT-IR devices, we used TSMRs to precisely assess the partition coefficients of the various VOCs. "Thermodynamic responses"—those directly proportional to the number of molecules in the film with a solely mass-dependent constant of proportionality—are generally obtained from acoustic wave devices supporting sorptive films that are acoustically thin.[29] This is typically an easier criterion to meet for the TSMR than for the SAW, because (a) the wavelength is longer for the TSMR, so a film can be thicker before it approaches a significant fraction of one acoustic wavelength and (b) the film is less deformed by the largely in-plane motion of the TSMR device surface, in contrast to the elliptically polarized motion of the SAW device surface.[29] As shown by Sauerbrey,[30] the vibrating frequency of a TSMR changes, to a first approximation, in proportion to the mass deposited onto or removed from the surface. Because both the analyte concentrations and the TSMR fundamental frequency are rather low (30 MHz), and the acoustic wavelength is fairly long (110 μm) compared to the coating thicknesses, viscoelastic effects are assumed to contribute little to the TSMR frequency change due to gas sorption.[31] Any changes in the conductivity of the sensing material would affect neither the SAW nor TSM device response, because in both cases the sensing film is deposited on a uniform gold film that shorts out the electric field associated with the acoustic wave.[28] Further details of acoustic wave-based mass-sensitive devices can be found in the literature.[28,31−33]

EXPERIMENTAL DETAILS

Coating Materials and Analytes. The coating materials chosen for this study (Figure 2) were as follows: a modified γ-cyclodextrin (3-*O*-butanoyl-2,6-di-*O*-*n*-pentyl-γ-cyclodextrin, CD)[34] as a cage compound, a nickel camphorate (nickel(II) bis[(1*R*)-(+)-3-(heptafluorobutanoyl)-8-methylidenecamphorate, Ni−Cam)[11] as a coordinatively unsaturated metal center, and a soluble nickel phthalocyanine (nickel 2,3,9,10,16,17,23,24-octakis(pentoxy)phthalocyanine, PC)[35] as a material with a large, delocalized π-electron system. CD and Ni−Cam were synthesized by the group of Prof. Schurig, and PC was synthesized by the group of Prof. Hanack, both at the Institute of Organic Chemistry of the University of Tübingen. In addition, we used the polar polymer poly(ether urethane) (PEUT; Thermedics, Woburn, MA)[9] and the nonpolar poly(isobutene) (PIB, MW ≈ 380 000; Aldrich, Milwaukee, WI) as conventional polymer coatings, nominally free of any molecular recognition moieties, for comparison.

The coatings on the SAW/FT-IR devices were prepared by spin casting from trichloromethane solutions or spray coating from dichloromethane solutions; layer thicknesses ranged from 500 nm to 1 μm. The TSMRs were coated with an airbrush using pure nitrogen as carrier gas. On-line monitoring of the frequency decrease allowed determination of the frequency shifts due to coating and calculation of the layer thickness, assuming a uniform and homogeneous distribution of the polymer over the device surface. The measured frequency shifts due to the coatings were approximately 50 kHz (thickness ∼250 nm).

Analytes and Vapor Generation. Most of the analytes were standard organic solvents, used as purchased from Sigma-Aldrich, Milwaukee, WI, without further purification. In addition, we used both enantiomers of methyl lactate (methyl 2-hydroxypropionate, purity >98%, Aldrich) and both enantiomers of methyl 2-chloropropionate (Fluka Chemie AG, Buchs, Switzerland).

Vapors were generated from specially developed temperature-controlled (T = 283−298 K) vaporizers using synthetic air as

(24) Crooks, R. M.; Sun, L.; Xu, C.; Hill, S. L.; Ricco, A. J. *Spectroscopy* **1993**, *8*, 28.
(25) Greenler, R. G. *J. Vac. Sci. Technol.* **1975**, *12*, 1410.
(26) Corn, R. Private communication.
(27) Thomas. R. C.; Hierlemann, A.; Staton, A. W.; Hill, M.; Ricco, A. J. *Anal. Chem.*, in press.
(28) Ballantine, D. S.; White, R. M.; Martin, S. J.; Ricco, A. J.; Frye, G. C.; Zellers, E. T.; Wohltjen, H. *Acoustic Wave Sensors: Theory, Design, and Physico-Chemical Applications*; Academic Press: San Diego, 1997.
(29) Martin, S. J.; Frye, G. C.; Senturia, S. D.*Anal. Chem.* **1994**, *66*, 2201.
(30) Sauerbrey, G. *Z. Phys.* **1959**, *155*, 206−222.
(31) Bodenhöfer, K.; Hierlemann, A.; Noetzel, G.; Weimar, U.; Göpel, W. *Anal. Chem.* **1996**, *68*, 2210.
(32) Grate, J. W.; Martin, S. J.; White, R. M. *Anal. Chem.* **1993**, *65*, 940A−948A, 987A−996A.
(33) Nieuwenhuizen, M. S.; Venema, A. *Sens. Mater.* **1989**, *5*, 261−300.
(34) König, W. A.; Krebber, R.; Mischnick, P. *J. High Resolut. Chromatogr.* **1989**, *11*, 732−738.
(35) Haisch, P.; Hanack, M. *Synthesis* **1995**, *19*, 1251.

carrier gas and then diluted as desired using computer-driven mass-flow controllers. The internal volume of these vaporizers, which distribute the liquid over a large-area packed-bed type support to maximize the surface to volume ratio, was dramatically smaller than that of typical gas-washing bottles ("bubblers"); hence very small quantities of expensive chiral analytes could be released at constant concentration.[36]

The absolute vapor-phase concentrations at the respective temperatures were calculated following the Antoine equation.[37] The analytes were vaporized at 293 K, whereas the measurement chamber and the sensors were maintained at 303 K. A p/p_0 value of 5% of, e.g., *n*-octane at 293 K hence corresponds to a p/p_0 value of 3% at 303 K (the proportionality factor depends on the analyte). Unless otherwise noted, p/p_0 values are corrected to 303 K, at which temperature the device and sensing film were maintained. All vapors were mixed and temperature-stabilized before entering the thermoregulated chamber. The gas flow rate was 200 mL/min for TSMR experiments and 500 mL/min for the SAW/FT-IR measurements, at a total pressure of 10^5 Pa.

Typical experiments consisted of alternating exposures to air or N_2 and vapor. The response time of the sensors is <1 s. Exposure times of 10 min were followed by 10 min purging of the chamber with synthetic air or N_2.

Thickness-Shear Mode Resonators and Surface Acoustic Wave Devices. The TSMR array consisted of discrete piezoelectric quartz crystals (AT-cut) with gold electrodes, operating at a fundamental frequency of 30 MHz (plate thickness: 55.6 μm), purchased from Kristallverarbeitung, Neckarbischofsheim, Germany.[31] Each crystal was powered by an oscillator circuit (bipolar, parallel resonance) constructed at the University of Tübingen; a single coaxial cable provides the supply voltage and transmits the frequency signal. A custom-developed scanner, compatible with signal frequencies between 100 kHz and 100 MHz, was controlled by a PCL 726 interface card (Labtech, Wilmington, MA) in an IBM-compatible PC-AT. This allowed for the sequential monitoring of each TSMR output by the computer using a Hewlett-Packard 5334B frequency counter interfaced via an IEEE-488 interface bus. Frequency differences, recorded every 30 s at 0.1 Hz resolution using a 1-s gate time, are reported relative to the initial, unperturbed value for each device. Sensor responses were taken as the frequency difference between analyte exposure and pure purge gas.

SAW delay-line devices were custom designed at Sandia National Laboratories to provide a large gold reflection area for the FT-IR measurements in the center of the interaction region of the SAW delay lines (Figure 3). Five independent sets of input and output interdigital transducers (IDTs; 200 nm thick Au on a 15 nm thick Cr or Ti adhesion layer) were defined on a 41 × 15.5 mm ST-quartz substrate. The IDT periodicity (acoustic wavelength) of 32 μm yields a center frequency of 97 MHz; each IDT is comprised of 50 finger pairs; the acoustic aperture of each device is 50 wavelengths; the center-to-center IDT spacing is 312 wavelengths. Compared to the SAW delay lines used in the past in our laboratory,[38] it was necessary to increase the center-to-center IDT spacing, in addition to using the large substrate that accommodates five identical delay lines, to provide a sufficiently large selective-film-coated Au reflection surface (8.5 × 40 mm in area, 200 nm of Au upon 15 nm of Ti or Cr) for the FT-IR-ERS measurements. Only the three center delay lines were used for SAW measurements. Adjacent (parallel) SAW delay lines are separated by 6.5 mm (200 wavelengths), and a detailed frequency analysis of the operating characteristics of these devices revealed negligible cross-talk. The response of the three independent SAW devices, therefore, could be measured simultaneously to provide redundant measurements during each analyte exposure. SAW measurements were performed according to previously described procedures.[18,38,39]

SAW/FT-IR-ERS Measurements. The combined SAW and FT-IR-ERS measurements were performed using a custom-designed test cell, Figure 3,[27] that fits onto a reflectance accessory for a commercial FT-IR spectrometer. The flow cell consists of two stainless steel body components. The cover section has six connectors allowing three independent SAW measurements, four O-ring-sealed window ports equipped with KBr windows, for 45°- and 80°-off-normal surface IR absorbance measurements, and two gas-flow ports. Spring-loaded "pogo" pins located at the bottom of this component make low-resistance contacts with the Au bonding pads of the SAW devices. The base section contains a recessed region to accurately locate the SAW/FT-IR-ERS device, as well as two liquid-flow connections to maintain the cell at a constant temperature during the measurements (303 K).

Measurements were performed using a Nicolet Magna-IR 750 spectrometer, including a KBr beam splitter and a liquid N_2-cooled $Hg_xCd_{(1-x)}Te$ (MCT) detector. Spectra were obtained using a Harrick Scientific (Ossining, NY) Seagull reflection accessory, configurable for surface reflection experiments at incident angles from 5 to 87° without optical realignment; the optical design results in no polarization dependence upon the angle of incidence. All spectra were acquired using an 80°-from-normal angle of incidence. The polarization of the incident IR radiation was set by a rotatable wire-grid polarizer. The following parameters were used to acquire the spectra: spectral range, 500−4000 cm^{-1}; aperture, 35 units (the dimension of these instrument-specific units are not available from the manufacturer); mirror velocity, 0.9494 m/s; resolution, 1 cm^{-1}; boxcar apodization; number of scans, 100; collection time, 160 s. The interferograms were saved for each spectrum to allow reprocessing of the spectra if desired.

For each molecular recognition coating material, several analytes expected to display specific chemical interactions were studied, and the results were compared to those for a number of nonspecifically sorbed analytes. For analytes of both categories, interactions with the "ordinary" organic polymers poly(isobutene) and poly(ether urethane) were also examined as controls. First, the gas-phase analyte spectra (under separate p and s polarization) were recorded at two different concentrations, using a bare gold reflecting surface in the SAW/FT-IR-ERS test cell (Figure 3). The reflection spectra of the bare gold surface under a nitrogen purge were subtracted as background. These gas-phase analyte spectra, which display essentially no difference between p and s polariza-

(36) Bodenhöfer, K.; Hierlemann, A.; Schlunk, R.; Göpel, W. *Sens. Actuators, B* **1997**, *45*, 259−264.

(37) Riddick, J. A.; Bunger, W. B.; Sakano, T. K. In *Organic Solvents*; Weissberger, A., Ed.; Techniques of Chemistry; Wiley-Interscience: New York, 1986; Vol. II.

(38) Ricco, A. J.; Frye, G. C.; Martin, S. J. *Langmuir* **1989**, *5*, 273.

(39) Thomas, R. C.; Sun, L.; Crooks, R. M.; Ricco, A. J. *Langmuir* **1991**, *7*, 620.

Table 1. TSMR-Derived Partition Coefficients in the Range $p/p_0 = 0-0.2\%$ for Analytes Sorbed into PIB, PEUT, CD, PC, and Ni−Cam Films

analyte	p_0 at 303 K (Pa)	partition coefficient[b]					normalized partition coeff[a]				
		PIB	PEUT	CD	PC	Ni−Cam	PIB	PEUT	CD	PC	Ni−Cam
n-octane	2430	1720 (30)	950 (30)	1780 (50)	720 (20)	250 (10)	1.0	1.0	1.0	1.0	1.0
toluene	4820	1030 (20)	1750 (20)	2400 (80)		650 (20)	1.2	4.1	2.7		5.2
trichloromethane	31900	200 (10)	850 (30)	1200 (50)	290 (10)		1.5	14	8.9	5.4	
tetrachloroethene	3160	2060 (30)	2050 (100)	2800 (150)	2100 (50)	810 (20)	1.6	3.2	2.1	3.9	4.3
propan-1-ol	3780	90 (5)	1380 (20)	1650 (50)	950 (30)	1600 (30)	0.1	2.2	1.5	2.1	10
methyl 2-*R*-chloropropionate	<500	860 (10)	3300 (50)	38000 (1300)			0.1	0.9	4.4		
methyl 2-*S*-chloropropionate	<500	860 (10)	3300 (50)	141000 (3500)			0.1	0.9	16		
R-methyl lactate	830	570 (20)	5400 (200)	83600 (2000)			0.1	2.7	16		
S-methyl lactate	830	570 (20)	5400 (200)	59000 (1500)			0.1	2.7	11		
benzene	15700	360 (10)	710 (20)		3500 (100)		1.4	5.4		32	
toluene	4820	1030 (20)	1750 (20)		11000 (500)		1.2	4.1		31	
m-xylene	1460	3400 (50)	5200 (200)		17500 (1000)		1.2	3.5		15	
pyridine	3570	480 (20)	3600 (200)		10200 (200)	37000 (1000)	0.4	5.8		21	220
tetrahydrofuran	29000	220 (5)	420 (20)		190 (10)	800 (30)	1.5	5.5		3.2	38
n-butylamine	15300	220 (10)	750 (20)			73000 (2000)	0.8	5.2			1800
pyrrole	1480	810 (20)	11500 (500)			3100 (100)	0.3	7.7			7.6
water (50% RH)	4180	- -	330 (5)	410 (20)		860 (20)		0.6	0.4		5.9

[a] Calculated from values in columns 3−7 by multiplication by p_0 and division by the value for *n*-octane. These normalized values from the TSMR may be compared to SAW data in Figures 5, 9, and 14. [b] Standard deviations are given in parentheses.

tions, served as references when searching for spectral changes due to specific analyte/coating interactions. The p and s spectra of all sensor coating materials were also recorded (under a nitrogen purge), subtracting the background reflection spectrum from a bare gold-coated device in each case. As expected, the bands associated with the films were much more intense for p-polarized spectra than for s, a consequence of the surface-selection rule. These coating spectra served as a second reference to determine whether any spectral changes observed upon analyte sorption were associated with the coating materials.

Next, s and p spectra were recorded for each analyte sorbed by each of the two "nonspecific" reference polymers, PIB (nonpolar) and PEUT (polar). The spectra of the analyte-free polymer-coated devices under a nitrogen purge were subtracted as background, eliminating all bands associated with the analyte-free polymer coatings. The resultant analyte spectra, which included contributions from the analyte in both gas and polymeric phases, were invariably identical in peak shapes, locations, and relative intensities to the analyte pure gas-phase spectra recorded using a bare gold reflecting surface, demonstrating the absence of any spectroscopically detectable specific interactions affecting either the analyte's or reference polymer's vibrational structure. Thus, in the IR spectra described below, spectra labeled PIB and PEUT are, in every case, identical to the gas-phase spectra of the respective analyte.

Finally, spectra were acquired for each of the analytes sorbed by each of the molecular recognition coatings. The sample spectra, which also included contributions from the analyte in both gas and polymeric phases, were then compared to the gas-phase spectrum of the respective analyte on the gold blank to detect any spectral changes. Sample spectra were acquired for at least three different concentrations of each analyte; concentrations were selected to achieve a reasonable IR signal intensity at the lowest possible gas-phase concentration, which, practically, meant that the absolute vapor-phase concentrations were adjusted to 3000−5000 ppm (by volume), regardless of the saturation vapor pressure, providing a roughly comparable IR absorbance from each analyte. The fraction of saturation vapor pressure (p/p_0) values at the vaporization temperature of 293 K hence ranged from 1% for trichloromethane to about 20% for tetrachloroethene, but all analyte concentrations were less than 10% of p_0 at the measurement temperature of 303 K. For each coating material, two independent SAW/FT-IR devices were prepared. After completing the set of measurements on one of the devices, a random sampling of analytes and concentrations was examined on the second device to confirm reproducibility of results.

RESULTS AND DISCUSSION

In the next sections, we discuss in detail the simultaneously recorded SAW and FT-IR-ERS data and the independently determined TSMR partition coefficients (summarized for all coating materials in Table 1) for each of the three different types of molecular recognition coating. Generally, major changes in the spectra are not expected, since all the specific interactions are completely reversible simply by removal of the analyte from the ambient phase (accomplished by purging with pure N_2). The interactions are cumulative physical and/or weakly chemical in nature; no chemical reactions occur; there are no severe distortions of the molecules, nor any strong, irreversible interactions.

Cage Compound: Modified γ-Cyclodextrin. Both enantiomers of methyl lactate and of methyl 2-chloropropionate were examined for specific (chiral) interactions with the CD; these were complemented by several reference analytes, expected not to interact specifically, but representing different chemical functionalities: *n*-octane, toluene, trichloromethane, tetrachloroethene, and propan-1-ol.

Figure 4 shows the relevant portions of the IR spectra of methyl lactate (i.e., methyl 2-hydroxypropionate) recorded simultaneously with the SAW response. From bottom to top, the absorbance spectra displayed are those of methyl lactate sorbed by PIB and PEUT ($p/p_0 = 2.7\%$; spectra are identical for R and S enantiomers), *S*-methyl lactate sorbed by CD ($p/p_0 = 2.7\%$), and *R*-methyl lactate sorbed by CD ($p/p_0 = 2.7$ and 5.4%). These spectral data have not been processed in any way.

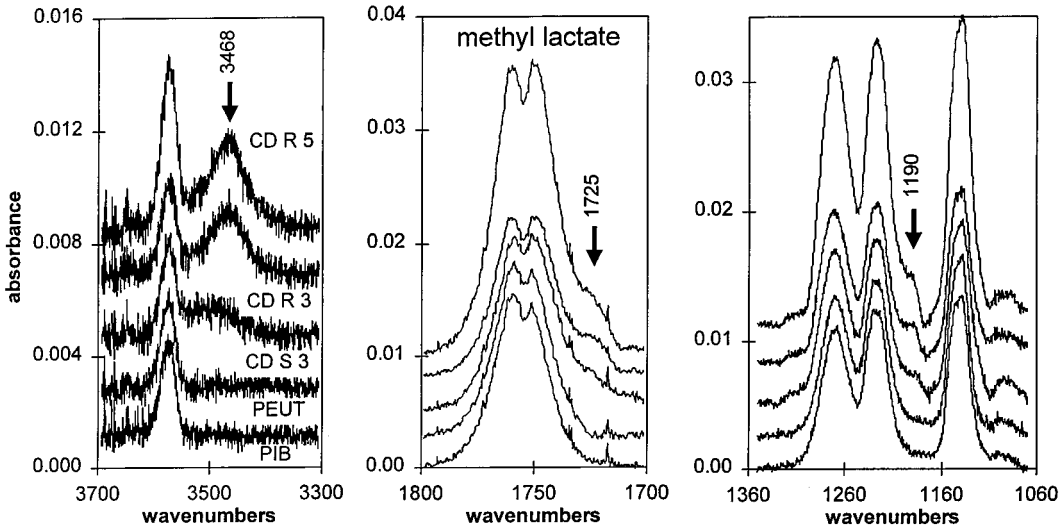

Figure 4. IR reflectance spectra of different concentrations of *R*-methyl lactate (p/p_0 = 5.4 and 2.7% at 303 K, CD R 5, CD R 3) and *S*-methyl lactate (p/p_0 = 2.7% at 303 K, CD S 3) sorbed by CD as well as by the reference polymers PIB and PEUT. Spectral changes are marked by arrows.

The spectra of methyl lactate sorbed in PIB and PEUT (Figure 4) are identical in peak shapes, locations, and relative intensities to the gas-phase spectra: simple physisorption does not affect the IR spectra. Three principal changes occur in the spectrum of methyl lactate sorbed by the CD (guidelines for interpreting IR spectra are given elsewhere[40–44]). First, a new peak appearing in the OH region around 3470 cm^{-1} (region of intermolecular hydrogen bonds) is much more pronounced for the R than the S enantiomer, consistent with the longer retention time of the R enantiomer on a GC column[9] and a larger response for this enantiomer from acoustic wave devices (see Figure 5 and Table 1). The peak maximum for the hydrogen bond of the S enantiomer is at 3488 cm^{-1}, that for the R enantiomer is at 3468 cm^{-1}, and the "regular" OH peak (gas-phase, free molecules) is at 3575 cm^{-1}. A similar H-bonding peak occurs for propan-1-ol interacting with the CD (not shown) at 3538 cm^{-1} (gas-phase OH peak at 3672 cm^{-1}) with a lower intensity than either methyl lactate enantiomer. Propan-1-ol, however, shows only a slightly increased partition coefficient with the CD relative to the reference polymers PIB and PEUT (from TSMR data; see Table 1).

Thus, the appearance of new vibrational bands suggests a specific interaction (H-bond-based bridging) but does not necessarily imply anomalously high partition coefficients. The intensity of such peaks offers a qualitative idea about the strength of the specific interactions, but our data do not reveal any simple, direct correlation between the number and/or intensity of these new vibrational bands and the magnitude of the partition coefficient. Comparing the intensities of spectral changes is likely to be most meaningful for very similar molecules, e.g., the two optical isomers of methyl lactate.

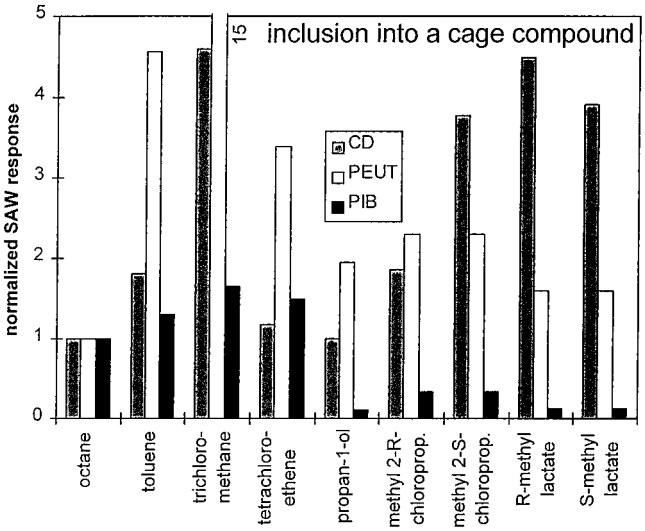

Figure 5. SAW sensor responses for coatings of the reference polymers PIB and PEUT and the highly selective cage compound CD upon exposure to various analytes, normalized to the responses to *n*-octane.

Badger et al. showed that the shift in the OH fundamental mode due to hydrogen bonding can be used as a measure of the strength of that bond, with a proportionality constant of about 8.5 $cm^{-1}/(kJ/mol)$.[45] Thus, the methyl lactate IR data, in which the OH peaks due to H-bonding between the CD and the two enantiomers differ by 20 cm^{-1}, imply a difference of 2.3 kJ/mol. This is comparable to the enantiomeric difference in Gibb's free energy of sorption determined by gas chromatography, 4 kJ/mol, indicating that the OH group contributes significantly to enantiomeric discrimination.

Further spectral changes for methyl lactate include a shoulder in the C=O stretching region at 1725 cm^{-1}, together with a slight change in the peak shape of the C=O peak (intensity increase on the low-energy flank) and a new peak or shoulder in the C−O stretching region at 1190 cm^{-1}. The intensity of these C−O and

(40) Fateley, W. G.; Dollish, F. R.; McDevitt, N. T.; Freeman, F. B. *Infrared and Raman Selection Rules for Molecular and Lattice Vibrations*; Wiley Interscience: New York, 1972.
(41) Bellamy, L. J. *Advances in Infrared Group Frequencies*; Methuen: London, 1958.
(42) Bellamy, L. J. *The Infrared Spectra of Complex Molecules*; Chapman and Hall: London, 1980.
(43) Colthup, N. B.; Daly, L. H.; Wiberley, S. E. *Introduction to Infrared and Raman Spectroscopy*; Academic Press: San Diego, 1990.
(44) Nakamoto, K. *Infrared and Raman Spectra of Inorganic and Coordination Compounds*, Parts A and B; Wiley-Interscience: New York, 1997.
(45) Badger, R. M.; Bauer, S. H. *J. Chem. Phys.* **1937**, *5*, 839.

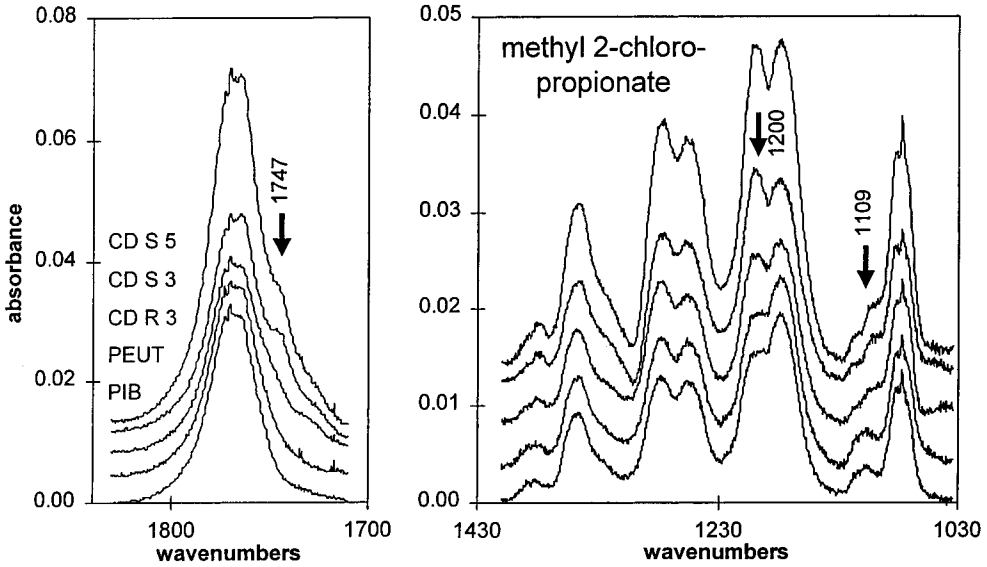

Figure 6. IR reflectance spectra of different concentrations of methyl 2-S-chloropropionate (p/p_0 = 5.4 and 2.7% at 303 K, CD S 5, CD S 3) and methyl 2-R-chloropropionate (p/p_0 = 2.7% at 303 K, CD R 3) sorbed by CD as well as by the reference polymers PIB and PEUT. Spectral changes are marked by arrows.

C═O changes again varies between R and S enantiomers, the changes in the R spectrum being the more pronounced, consistent with its stronger sorption by the CD matrix.[9]

Intriguing results are obtained for an analyte identical to methyl lactate, save for the replacement of the −OH by a −Cl group in the "2" position. The IR spectral changes associated with the sorption of methyl 2-chloropropionate are shown in Figure 6, from bottom to top: reference polymer spectra (PIB, PEUT, p/p_0 = 2.7%); R enantiomer (p/p_0 = 2.7%); S enantiomer (p/p_0 = 2.7 and 5%). In contrast to the H-bonding results for methyl lactate, sorption of the two enantiomers of methyl 2-chloropropionate by the CD causes no changes in the C−Cl (560−830 cm^{-1}) or H−Cl (2600−3100 cm^{-1}) spectral regions, indicating no analogous intermolecular hydrogen bonds. This is not at all surprising, since the CD has no significant H-bond donor sites to interact with the Cl, but nonetheless it may help explain why there is an inversion in the elution order for GC columns,[9] as well as a reversal of the relative acoustic wave sensor signal magnitudes (Figure 5, Table 1), in going from methyl lactate, for which R interacts more strongly than S, to methyl 2-chloropropionate, for which the converse is true.[9]

As in the case of the structurally very similar methyl lactate, a shoulder appears on the C═O stretch at 1747 cm^{-1} for both chloropropionate enantiomers (Figure 6). However, consistent with the inverted enantiomeric preference, this shoulder is more pronounced for the S than the R enantiomer. In addition, Figure 6 shows a remarkable variation in the peak intensity in the C−O stretching region at 1200 cm^{-1} (compared to the neighboring peak at 1179 cm^{-1}) and the disappearance of the shoulder at 1109 cm^{-1} (the C−O stretch of C−OR). The changes in the C═O and C−O regions for both methyl lactate and methyl 2-chloropropionate support our previous speculation that the presence of a methoxy, halogenated methoxy, or ester group promotes preferential sorption in the CD torus.[9] This is believed to result from the methoxy functionality being the proper size and shape to fit snugly into the central region of the torus, a hypothesis supported by a measured stoichiometry between CD and either of the propionates of approximately 1:1 (in the low-concentration "Langmuirian" sorption regime).

When interpreting the spectral changes for the propionates, one must also take into consideration the fact that the CD itself has a C═O absorbance at 1758 cm^{-1} and a C−O absorbance at 1179 cm^{-1}. Hence, the observed spectral changes associated with those functionalities could arise from a shift of the bands of either the analyte *or* the CD (or perhaps both) due to the specific interactions. However, similar spectral changes have been recorded for the anesthetics enflurane and isoflurane sorbed by the same CD used in this work.[46] These changes, measured using attenuated total internal reflection IR, affect mainly the C−F bands of the two anesthetics and therefore cannot be spectral changes in the CD. This report, coupled with the fact that the CD molecular cage is not particularly rigid and is relatively large compared to the analyte molecular dimensions, allowing minor conformational changes with little energetic penalty, leads us to believe that the C═O and C−O vibrational changes in Figures 4 and 6 are associated with the analytes.

Another feature of the spectral changes of both propionates interacting with the CD is saturation in absorbance intensity as analyte concentration increases: the new OH peak of methyl lactate, or the C−O stretch change of methyl 2-chloropropionate, for example, has nearly achieved maximum intensity at p/p_0 = 2.7%. Upon increasing the analyte concentration to 5.4% (top spectrum) or 10.8% of saturation (not shown), the "regular" OH peak (gas phase, no H bonds) for methyl lactate at 3575 cm^{-1} gains much more intensity than the shoulder at 3468 cm^{-1}; the same holds true for the changes in the C−O stretching region (1200 and 1179 cm^{-1}) of methyl 2-chloropropionate. This saturation of the signal, which has been observed by other authors as well,[10] results from the limited number of preferential sorption sites available in the coating: the intensity of the changes caused by this preferential sorption attains its maximum when all such sites are occupied. For the propionates interacting with the CD,

(46) Kramer, M. Ph.D. Dissertation, University of Tübingen, 1997.

this occurs near $p/p_0 = 2\%$. From TSMR investigations, at most 80% of all the cyclodextrin molecules are accessible to the analyte.[9]

Finally, we note that no spectral changes were observed for either the analytes or the CD upon coating exposure to *n*-octane, toluene, trichloromethane, or tetrachloroethene. This confirms that spectral perturbation is not invariably associated with sorption of an analyte by the CD, even for cases such as trichloromethane, in which SAW results show a response signal comparable to that for the propionates.

SAW responses recorded concurrently with the IR measurements for the CD and the two reference polymers are summarized in Figure 5 for exposure to the two propionates (both enantiomers of each) as well as the set of "reference" solvents (*n*-octane, propan-1-ol, toluene, trichloromethane, and tetrachloroethene). The frequency shifts (three different concentrations per analyte) of each of the three delay lines constituting one of the SAW/IR devices were normalized by dividing by the p/p_0 and molecular weight of the analyte. Normalization for p/p_0 was done over a fairly narrow range of concentrations, where the response was approximately linear with concentration. These responses were further normalized to the magnitude of the response from *n*-octane for each delay line, to compensate for differences in coating thickness among the three delay lines distributed over this relatively large device. Finally, all of the normalized responses for a given analyte were averaged to yield one datum per analyte/coating combination. These average values are characterized by a standard deviation that is some 10−20% larger than for "ordinary" SAW delay lines operating at the same frequency (the latter having 230 wavelength IDT spacing rather than 312 for the SAW/IR devices).

Normalization of sensor signals for analyte vapor pressure (which is typically a good estimate of fugacity, particularly well below saturation) allows thermodynamic comparisons to be drawn between the responses to different analytes, within the limits of any analyte- or concentration-dependent viscoelastic effects. In the event that sensor response depended only upon analyte thermodynamic activity (fugacity), all the responses in Figure 5 would be approximately equivalent, as would all the normalized partition coefficients reported in Table 1. Within a factor of approximately 2, such behavior is found for PIB for the analytes octane, toluene, trichloromethane, and tetrachloroethene for both the SAW (Figure 5) and TSMR (Table 1) responses. For the more polar analytes, the nonpolar PIB has considerably less affinity. For the more polar polymer PEUT, deviations from a pure p/p_0 response are significant for nearly all analytes.

In the event that pronounced molecular recognition leads to anomalously large partition coefficients for some analytes, the corresponding bars in the graph of Figure 5 should stand out from the rest. This seems to be the case for the propionates, although not to the extent expected (compare Table 1). At least part of the reason for this is straightforward: to have enough analyte in the film for measurable spectral changes to be recorded, we found it necessary to use a minimum vapor concentration of about 2% of p/p_0. This, unfortunately, is in the region of the sorption isotherm (Figure 1) where saturation of most of the selective sites has already occurred, and the slope is consequently decreasing; the response in this regime is, in significant measure, Henry's law behavior. The TSMR partition coefficients in Table 1, however,

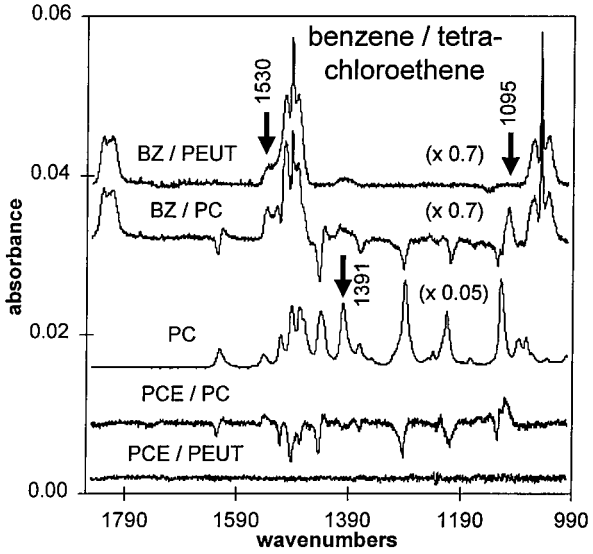

Figure 7. IR reflectance spectra of benzene ($p/p_0 = 3.1\%$ at 303 K, BZ, multiplied by 0.7) and tetrachloroethene ($p/p_0 = 5.8\%$ at 303 K, PCE) sorbed by PC and the reference polymer PEUT. The spectrum of pure PC (PC, multiplied by 0.05) is given for comparison. Spectral changes are marked by arrows.

are determined according to ref 31 from the initial slope at very low concentrations and therefore show the preferential sorption more dramatically. Both SAW and TSMR[9] sensor results show a clear discrimination of the enantiomers (signal intensity variations are consistent with elution order in GC) of both pairs of the propionates. Both sensor platforms also show large responses to trichloromethane. Besides the different concentration ranges used for the determination of the SAW and TSMR response (p/p_0 at least 2−5% for the FT-IR/SAW, but below 0.2% for the TSMR), further relative discrepancies between SAW and TSMR results are probably due in significant measure to the fact that SAW responses are, for some materials in some thickness ranges, significantly more sensitive to viscosity and modulus effects.

π-Stacking: Nickel Phthalocyanine. Here, chemical specificity is expected to result from an intense interaction of the large, delocalized π-electron system of the phthalocyanine with easily polarizable electron systems (bromine, iodine, etc.) and with unsaturated π-bonded compounds (alkenes, etc.); but the strongest interactions are expected with π-electron-containing aromatic ring compounds. Figure 7 shows, from bottom to top, the spectra of tetrachloroethene sorbed in PEUT and PC ($p/p_0 = 5.8\%$), the reflection absorption spectrum of the pure PC, and the spectra of benzene in PC and PEUT ($p/p_0 = 3.1\%$). Figure 8 shows the spectra of toluene: $p/p_0 = 1.2$ and 3% in PC, as well as $p/p_0 = 1.2\%$ in PIB and PEUT. Again, the spectra recorded for the PEUT and PIB coatings are identical to those of the pure solvent vapor. The most obvious changes in the spectra when PIB or PEUT is compared to PC are a number of "negative" peaks arising at frequencies characteristic of the PC absorbance spectrum (Figure 7; the spectra of most metal phthalocyaninato complexes are very similar; see, e.g., refs 47 and 48). This is most clear in the case of tetrachloroethene (Figure 7), which has no characteristic absor-

(47) Kalz, W.; Homborg, H. *Z. Naturforsch.* **1983**, *38b*, 470.
(48) Sievertsen, S.; Schlehahn, H.; Homborg, H. *Z. Anorg. Allg. Chem.* **1993**, *619*, 1064−1072.

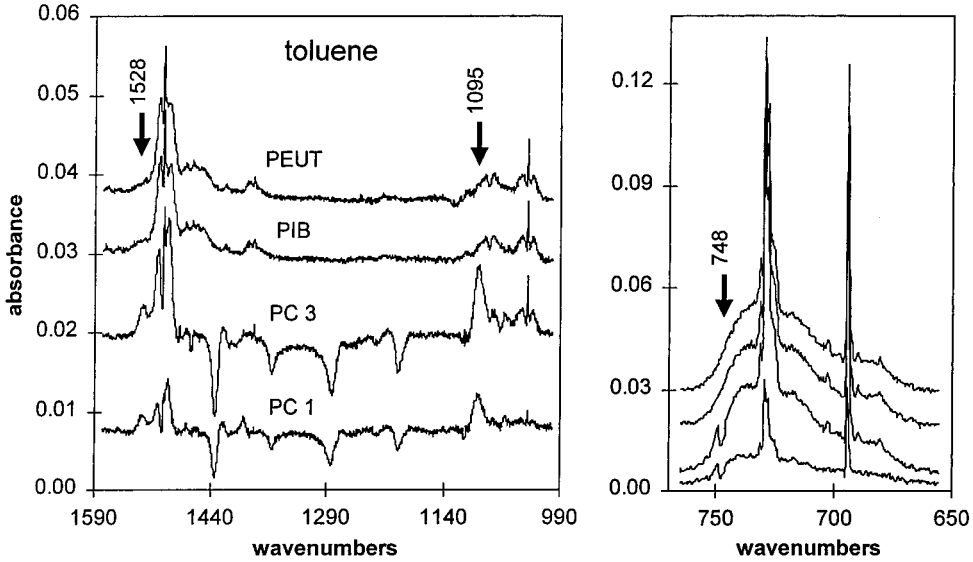

Figure 8. IR reflectance spectra of different concentrations of toluene (p/p_0 = 1.2 and 3% at 303 K, PC 1, PC 3) sorbed by PC and the reference polymers PIB and PEUT (p/p_0 = 3% at 303 K). Spectral changes are marked by arrows.

bance in this (aromatic) spectral region, but also occurs in the case of benzene.

There are several possible explanations for the decrease in intensity of the PC peaks upon exposure to the analyte vapor. One is that the effective optical path length through the PC film decreases as a consequence of a change in refractive index, which could result from a perturbation of the PC's electronic structure, particularly that associated with the aromatic structure, by the π-stacking process. The PC, as well as the nickel camphorate (discussed below), are deposited as polycrystalline thin films. It is possible, therefore, that insertion of π-stacking analytes between adjacent phthalocyanines could affect the morphology or packing of the crystallites, thereby altering the optical parameters.[49] It is significant that no comparable effects were observed for any of the polymers or the "oily" CD layer; only the polycrystalline materials show such effects. No such negative peaks were observed as a result of the sorption of *n*-octane, trichloromethane, or propan-1-ol.

For the unsaturated compound with the smallest π system of those examined, tetrachloroethene, the negative peaks are relatively weak, Figure 7. Besides the small negative PC peaks, the other spectral changes associated with the sorption of tetrachloroethene by PC are a small positive peak at 1095 cm^{-1} and the absence of a negative peak at 1391 cm^{-1}.

For benzene (Figure 7), toluene (Figure 8), *m*-xylene, and pyridine, the negative peaks resulting from sorption by the PC have considerable intensity. It is remarkable that the PC peak at 1391 cm^{-1} (associated with C−H deformations) does not also occur as a negative peak; the reason for this is not clear. For all four aromatic compounds, as well as tetrachloroethene, a characteristic peak appears at 1095 cm^{-1} (Figures 7 and 8). Since this peak has precisely the same frequency for all five π compounds, it probably originates from the phthalocyanine. In the absence of analyte, the PC has a set of bands at 1065 and 1105 cm^{-1} (Figure 7), which are characteristic of the metal coordination state.[48] It seems likely, therefore, that upon adsorption to the PC system, the aromatics either (partially) occupy the free coordination sites of the metal (the PC complex is planar) or influence the PC donor bonds to the metal. Further evidence for the important role of the metal is provided by the sensor responses for the PCs, which decrease drastically when two axial ligands are introduced, or no metal central atom (2 H atoms instead) is present.[12] Unfortunately, the reflection IR technique does not allow the study of the 100−500 cm^{-1} region, where the ring deformation bands of the phthalocyanine and the $M-N_4$ stretching bands are located.[52]

Another significant spectral change occurs in the ring-breathing-mode region of benzene, toluene, and *m*-xylene. A shoulder appears on the high-energy flank of the ring-breathing peak at 1530 cm^{-1} for benzene (Figure 7) and at 1528 cm^{-1} for toluene (Figure 8) and *m*-xylene (not shown). The symmetry of this ring-breathing peak is clearly altered, but in the case of benzene this might result from superposition of this peak (1484 cm^{-1}) with the negative peaks discussed above (see Figure 7). In the case of toluene (Figure 8) and *m*-xylene (not shown), the ring-breathing modes are shifted to somewhat higher frequency (1501 cm^{-1}) and, hence, there is no interference from the negative peaks. Also for toluene and *m*-xylene, we observe changes in the peak shape

(49) A less likely explanation also derives from the polycrystalline structure of the PC and nickel camphorate. Since polycrystalline materials are densely packed in the crystalline domains, insertion of the analyte molecules into those domains could actually reduce the physical density of the coatings in the near-surface region probed with enhanced sensitivity by the p-polarized IR beam; consequently, negative peaks could occur. (In contrast, the polymers and the CD have considerable free volume and should not be similarly affected.) In every case where this effect was observed, the negative peaks, along with any other spectral changes, are much less pronounced in the s- than the p-polarized spectrum. Since the reflective layer is gold, since the negative peaks are attributable to simple decreases in absorbances of the coating materials and do not show derivative-like characteristics, and since the p and s spectra show the same alterations (no ordering effects), we believe that the distortion of spectral band shapes by optical effects and related phenomena (see refs 23, 50, and 51) need *not* be taken into account here.

(50) Porter, M. D.; Karweik, D.; Kuwana, T.; Theis, W.; Norris, G. B.; Tiernan, T. O. *Appl. Spectrosc.* **1984**, *38*, 11−16.

(51) Schlotter, N. E.; Porter, M. D.; Bright, T. B.; Allara, D. L. *Chem. Phys. Lett.* **1986**, *132*, 93−98.

(52) Terzian, G.; Moubaraki, B.; Mossoyan-Deneux, M.; Benlian, D. *Spectrochim. Acta* **1989**, *45A*, 675−677.

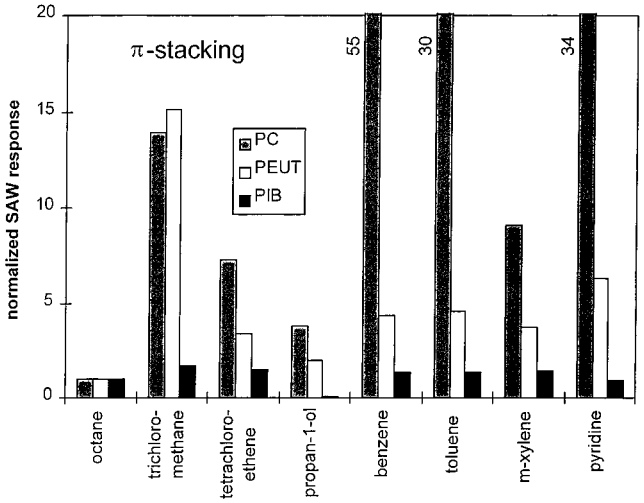

Figure 9. SAW sensor responses for coatings of PC and the reference polymers PIB and PEUT upon exposure to various analytes, normalized to the responses to *n*-octane.

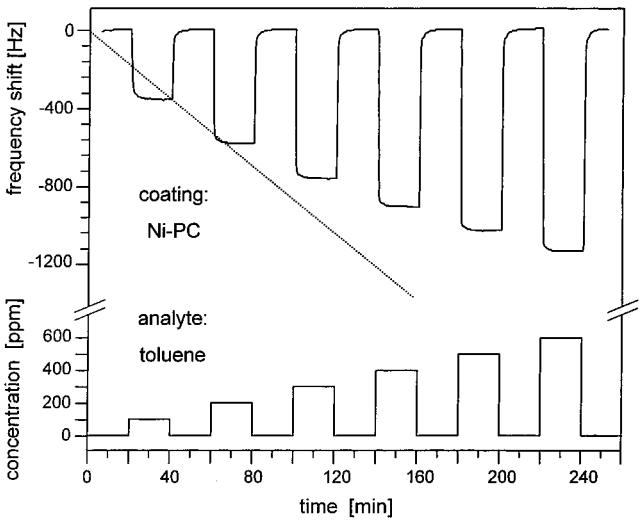

Figure 10. Sensor signals of a 30-MHz TSMR coated with PC upon exposure to different concentrations of toluene. The dotted line marks a hypothetical linear correlation.

(dips) of the out-of-plane deformation of ring H atoms; these very intense peaks are located at 729 cm^{-1} for toluene and 770 cm^{-1} for *m*-xylene.

Consistent with the smaller spectral changes compared to benzene, toluene, *m*-xylene, and pyridine, the tetrachloroethene sorption isotherm is linear and the partition coefficients are not nearly as large as those of the aromatic ring compounds (Figure 9, Table 1). In contrast, the four aromatic ring compounds exhibit nonlinear sorption characteristics and significantly increased partitioning in the nickel−phthalocyanine matrix (Figure 9, Table 1). The bars representing the PC-coated SAW-device responses to the aromatics stand out markedly in Figure 9. The large response to trichloromethane might be a result of interactions between the PC π-cloud and the polar trichloromethane.

The sensor response from a PC-coated TSMR, upon exposure to toluene, is shown in Figure 10. Although the coating material is polycrystalline, the sensor response is rapid and a stable equilibrium state is reached quickly at each concentration. The low noise of the sensor signal and the stability of the baseline

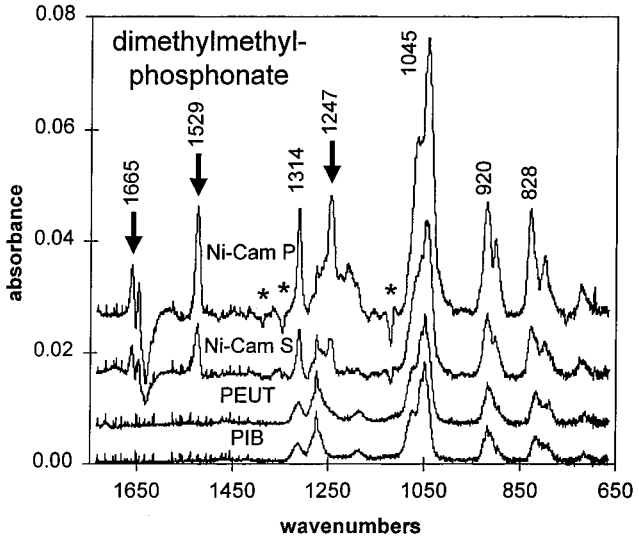

Figure 11. IR reflectance spectra of dimethyl methylphosphonate (DMMP; p/p_0 = 5.5% at 303 K) sorbed by Ni−Cam using different beam polarizations (Ni−Cam P, Ni−Cam S) and sorbed by the reference polymers PIB and PEUT. Spectral changes are marked by arrows. The asterisks mark negative peaks corresponding to Ni−Cam absorbances.

are also notable in Figure 10. The response as a function of concentration is clearly nonlinear (as in the isotherms of Figure 1), consistent with a dual-mode sorption process, characteristic of specific chemical interactions, as discussed in the introduction. Analogous modeling and fitting of the PC isotherms as discussed in detail in ref 9 was done for the PC.[12]

Metal Coordination: Nickel Camphorate. Due to the nature of coordinative ligand−metal donor bonds, the spectral changes are expected to be more pronounced for the transition metal camphorate complex (see Figure 2) than in the case of the CD and the PC. Note that the two water ligands are weakly bound, so this complex is effectively coordinatively unsaturated, and therefore readily binds Lewis bases. Earlier TSMR investigations revealed fully reversible but slow sensor response characteristics, along with a significantly enhanced interaction energy relative to conventional polymers;[11] the enrichment of the analyte in the bulk coating material is therefore expected to be relatively high. Since the nickel camphorate is polycrystalline like the PC, the same considerations discussed in the previous section hold for the "negative" spectral peaks associated with Ni−Cam upon sorption of some analytes. Fortunately, Ni−Cam has only a few absorbances of low intensity in the spectral regions of interest, as detailed below.

Dimethyl methylphosphonate (DMMP) was selected as an oxygen-containing σ-donor ligand. Figure 11 shows the spectra of p/p_0 = 5.5% DMMP in PIB, PEUT (*p*-polarized spectra, which are identical to the gas-phase spectra), as well as the s and p spectra for DMMP sorbed by Ni−Cam. As expected, the spectral changes are more intense in the surface-sensitive p-polarized spectrum. The enhanced sorption (peak intensity) in the Ni−Cam, as compared to the reference polymers, is apparent. In addition to an appreciable increase in the intensity of most of the peaks and a few negative peaks (marked with asterisks), there are three major changes in the spectra. From left to right, the first significant change occurs in the C=O region. Ni−Cam has a C=O absor-

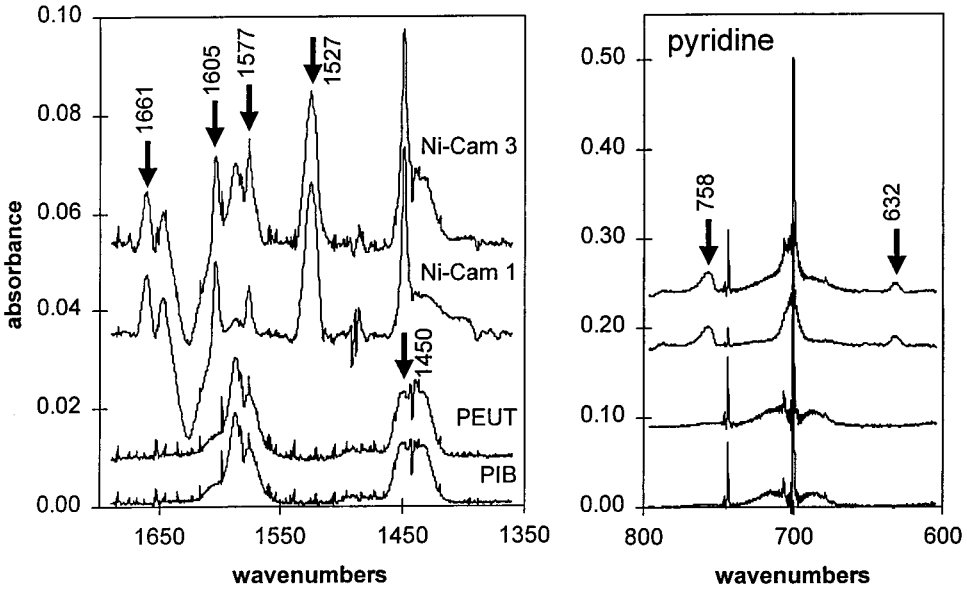

Figure 12. IR reflectance spectra of different concentrations of pyridine (p/p_0 = 1.1 and 2.9% at 303 K, Ni−Cam 1, Ni−Cam 3) sorbed by Ni−Cam and the reference polymers PIB and PEUT (p/p_0 = 2.9% at 303 K). Spectral changes are marked by arrows.

bance at 1640 cm^{-1}. A large "dip" is recorded at 1636 cm^{-1}, and two new peaks appear at 1650 and 1665 cm^{-1}. The dip may be partially attributable to a negative peak, but compared to the intensity of the other negative peaks, it is probable that there are additional structural changes responsible for this change: the β-diketonate coordination to the Ni appears to undergo changes upon coordination of the phosphonate to the Ni. The β-diketonate and Ni form a delocalized π-system (β-diketonate acts as a σ electron donor and π-acceptor for the coordinative bonds).[11] Upon coordination of the phosphonate ligand, the Ni receives additional σ-electron density from this new donor, but probably also back-donates to the P═O π-system, hence reducing the electron density that is back-donated to the C═O π-bonds. Because the C═O π-bonds are predominantly antibonding in character, diminishing the back-donation into these bonds enhances the overall strength of the C═O bond, shifting it to higher energy (wavenumber).[53] This, we believe, is responsible for the two new bands at 1650 and 1665 cm^{-1}, in addition to and contributing to the dip at 1636 cm^{-1}. (For comparison, the C═O bands of the uncoordinated free camphorate are at 1700 cm^{-1}).

Related to the change in the C═O bands is the appearance of a peak at 1529 cm^{-1}, which also can be attributed to changes in the β-diketonate−nickel system: it is characteristic of the combination of C═O and C═C in the aromatic system of the Ni−Cam.[44,54] The increased intensity of this peak indicates changes in this aromatic system, specifically decreased back-donation of the Ni into the aromatic system as already described. Both the changes in the C═O region and the peak at 1529 cm^{-1} are characteristic of the camphorate and should occur upon exposure to any specifically recognized analyte (compare Figure 13 for a nonspecific analyte).

The third set of obvious changes is related to the phosphonate analyte. The P═O stretch at 1276 cm^{-1} has the same intensity for sorption by PIB or PEUT (equivalent to gas-phase DMMP spectra) as those for the s and p spectra of the camphorate. This band is therefore assigned to the P═O stretch of the free vapor-phase molecule, since the gas-phase concentration is identical for all coatings. Near this band, however, a new peak arises exclusively for the Ni−Cam coating at 1247 cm^{-1} (also in the P═O region) due to the Ni-coordinated phosphonate. This bathochromic shift of nearly 30 cm^{-1} relative to the free phosphonate supports the hypothesis presented above in the discussion of the C═O band shift, namely, that some of the Ni π-electron density is back-donated to the antibonding π-levels of the P═O bond, weakening it as a result. The appearance of the weakened P═O band at 1247 cm^{-1} suggests significant interaction between Ni and the phosphoryl oxygen. In addition, there are several minor spectral changes in the phosphonate spectrum: the P−CH_3 symmetric deformation at 1314 cm^{-1} increases in intensity, the asymmetric P−O−C stretch shifts slightly from 1052 to 1045 cm^{-1}, the symmetric P−O−C stretch shifts slightly from 819 to 828 cm^{-1}, and the P−CH_3 rock at 920 cm^{-1} develops a new shoulder. All these peaks gain intensity, since the positions of the original gas-phase peak and the peak of the absorbed species are at the same or very similar frequencies. The only gas-phase peak that differs in frequency from the adsorbed species enough that it gains no intensity is the P═O peak at 1276 cm^{-1}.

The affinity of DMMP for this coordinatively unsaturated Ni complex has parallels to our work on the selective detection of a closely related organophosphonate, diisopropyl methylphosphonate (DIMP). Self-assembled monolayers terminated by coordinately unsaturated copper resulted in selective binding of DIMP using the SAW platform.[18,55] Further, an extensive IR reflectance study revealed similar effects on the bands characteristic of the phosphonate upon reversible coordination of the DIMP.[56]

The spectra associated with the sorption of a nitrogen-containing aromatic compound, pyridine, are shown in Figure 12.

(53) Avanzino, S. C.; Bakke, A. A.; Chen, H.-W.; Donahue, C. J.; Jolly, W. L.; Lee, T. H.; Ricco, A. J. *Inorg. Chem.* **1980**, *19*, 1931.
(54) Mikami, M.; Nakagawa, I.; Shimanouchi, T. *Spectrochim. Acta* **1967**, *23A*, 1037.
(55) Kepley, L. J.; Crooks, R. M.; Ricco, A. J. *Anal. Chem.* **1992**, *64*, 3191.
(56) Crooks, R. M.; Yang, H. C.; McEllistrem, L. J.; Thomas, R. C.; Ricco, A. J. *Faraday Discuss.* **1997**, *107*, 285.

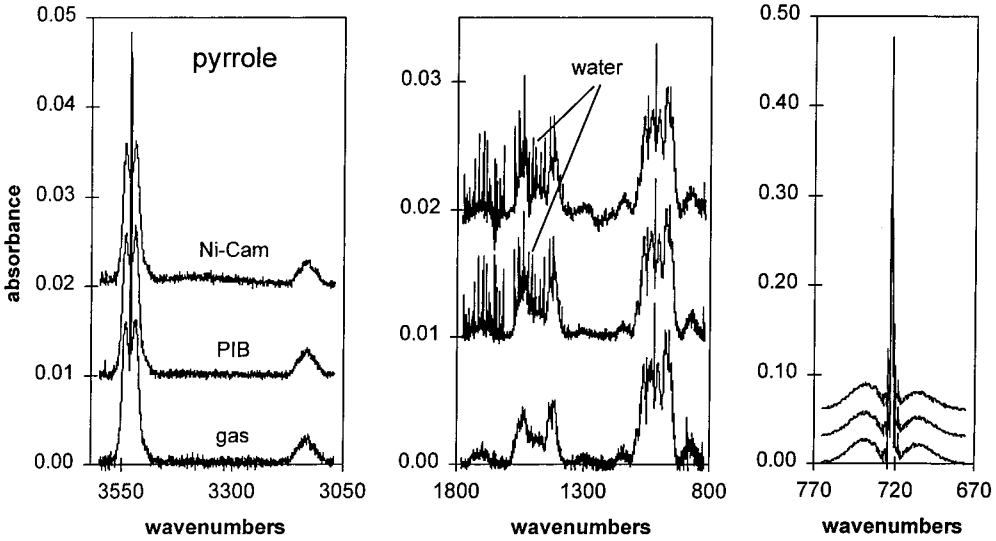

Figure 13. IR reflectance spectra of pyrrole (p/p_0 = 5.3% at 303 K) using a gold blank (vapor) and absorbed into Ni−Cam and into the reference polymer PIB. No spectral changes occur. Spectral lines resulting from contamination of the pyrrole source with water are indicated.

The *p*-polarized spectra of PIB and PEUT upon exposure to 2.9%-of-saturation pyridine and the *p* spectra of Ni−Cam upon exposure to 1.1 and 2.9% pyridine are depicted. It is notable that the enrichment of the analyte (as indicated by the analyte IR peak intensity) in the coating is not as pronounced as in the case of DMMP. This is due to the higher saturation vapor pressure of pyridine as compared to DMMP. Again, spectral changes related to the camphorate are observed: a dip at 1626 cm^{-1} and two new peaks at 1647 and 1661 cm^{-1} in the C═O region, and a new peak in the region of the aromatic nickel−β-diketonate system at 1527 cm^{-1}. In analogy to the situation described above for the phosphonate and Ni−Cam, the appearance of the two C═O peaks at higher energy is consistent with the π-system of the pyridine accepting π-back-donation from the Ni, lessening the amount of donation to the antibonding C═O π system, thereby strengthening that bond.

The gas-phase (or PIB or PEUT) spectrum shows mainly a doublet at 1588 and 1577 cm^{-1}, as well as a double peak at 1448 and 1436 cm^{-1}, all of which can be assigned to ring-breathing modes of the pyridine. In the Ni−Cam spectra, the symmetry of the 1448/1436 cm^{-1} pyridine double peak is clearly altered, the high-frequency peak at 1450 cm^{-1} increasing markedly in intensity. In the 1.1% Ni−Cam spectrum, these changes are even more obvious, since the gas-phase signals are still comparably small. As the analyte concentration increases from 1.1 to 2.9%, the right side of the double peak increases to somewhat more than in the gas-phase or reference polymers, while the peak at 1450 cm^{-1} grows only slightly. The other changes occur in the 1577/1588 cm^{-1} doublet. The peak at 1577 cm^{-1} is intensified, thus changing the symmetry of the doublet, and a new peak at 1605 cm^{-1} appears clearly in the 1.1% spectrum. Increasing the gas-phase concentration of pyridine from 1.1 to 2.9% causes the intensity of the gas-phase 1588/1577 cm^{-1} doublet to increase correspondingly. The changes in this spectral region upon increasing the pyridine concentration from 1.1 to 2.9% are reminiscent of the saturation behavior discussed above for the CD coating: as soon as the preferential sorption sites have been occupied, the intensity of the spectral changes due to preferential sorption increases no further. The concentration limit at which such saturation effects occur depends strongly upon the vapor pressure of the analyte and the site/analyte interaction energy.

The changes in the region of the ring-breathing modes indicate that the symmetry and the electron-density distribution of the aromatic ring system change upon coordination of the N atom to the Ni. Further changes occur in the regions of out-of-plane C−H deformations (745 cm^{-1}) and ring deformations (701 cm^{-1}). In addition, two new satellite peaks appear at 758 and 632 cm^{-1}, and the shape of the ring-deformation peak at 701 cm^{-1} changes, giving further indication of changes in the ring-breathing region.

For *n*-butylamine (spectra not shown), we find, in addition to the changes related to the camphorate, changes in the NH_2 stretching and wagging regions: a new peak appears at 3280 cm^{-1}, shifted to lower frequency relative to the original NH_2 stretch of the gas-phase molecule at 3347 cm^{-1}, and a shoulder appears at 739 cm^{-1} on the low-energy flank of the NH_2 wag at 780 cm^{-1}. The new NH_2 stretching peak is close to that of a secondary amine, consistent with coordination of the primary amine group to the Ni; the same holds for the shoulder on the NH_2 wag. A similar shift can be observed for the C−N stretch: a new peak occurs at 1023 cm^{-1}, shifted from the 1088 cm^{-1} C−N stretch observed in the gas-phase (or PIB) spectrum.

The weakly coordinating oxygen-containing compounds propan-1-ol and tetrahydrofuran (THF) show changes in the spectral bands of the camphorate, but no other changes; coordination may be too weak to affect the spectra of these ligands. No changes at all were observed upon exposure to toluene, octane, tetrachloroethene, trichloromethane, and, perhaps surprisingly, pyrrole.

The spectra of pyrrole (vapor, sorbed in PIB, sorbed in Ni−Cam; p/p_0 = 5.3%) are shown in Figure 13. There are no spectral changes relative to the gas-phase spectrum for either coating. The series of closely spaced peaks in the 1500−1800 cm^{-1} region result from water absorbed into the vapor source (a gas washing bottle). Pyrrole has a nitrogen atom and is heteroaromatic; the free electron pair of the nitrogen is part of the aromatic system; therefore, the Lewis basicity of the N, and hence its ability to donate electrons into a coordinative bond with the Ni atom, are

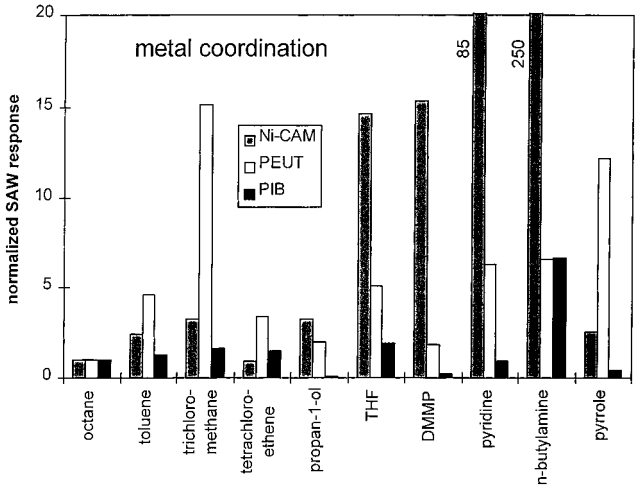

Figure 14. SAW sensor responses for coatings of the reference polymers PIB and PEUT and the metal coordination compound Ni–Cam upon exposure to various analytes, normalized to the responses to *n*-octane.

quite low (there is even a positive dipole charge on the N atom): pyrrole is a very poor electron donor or ligand.

The acoustic wave sensor data, presented in Figure 14 and Table 1, are consistent with the IR results discussed above. Increases in the sensor signals were recorded for the weakly coordinating oxygen-containing compounds THF and DMMP, with fairly remarkable enhancement of the signal for the nitrogen-containing compounds pyridine and *n*-butylamine, both good Lewis bases. Consistent with the absence of any spectral changes in the case of pyrrole, neither the sensor signals (Figure 14, Table 1) nor the GC retention time for this molecule are enhanced in comparison to the reference polymers PIB and PEUT.[11] Again, the occurrence of spectral changes is closely correlated to anomalously high partition coefficients.

CONCLUSIONS

The method of simultaneous SAW/in situ FT-IR measurements is an effective, powerful tool for elucidating interactions between coatings and gaseous analytes, providing direct evidence for specific interactions between volatile analytes and coating materials on acoustic wave gas sensors. Our SAW/FT-IR results support earlier conclusions derived from TSMR data[9,11,12] regarding the molecular specificity of several thin-film materials. In most cases where specific chemical interactions—here including metal coordination, cage-compound formation, and π-stacking—are expected, we record distinctive, assignable changes in the IR spectra, together with anomalously large SAW sensor responses, upon analyte dosing.

In contrast, for ordinary physisorption processes, exemplified by the conventional organic polymers PEUT and PIB interacting with various volatile organic compounds, no changes in the IR spectra occur, and SAW responses are smaller; the partition coefficients tend roughly to follow the fraction of saturation vapor pressure, although significant variations occur, particularly when comparing the nonpolar poly(isobutene) to the polar poly(etherurethane).

From the results presented in this paper, we conclude that the process of "molecular recognition" in chemical sensors, although it has been a source of some controversy in the literature, is generally viable. The related effects and selectivities, however, often may prove to be smaller than hoped, and can be observed almost exclusively at low analyte concentrations. At high analyte concentration, nonspecific sorption or physisorption invariably dominates. The definition of "low" concentration depends on the interaction energy for a particular analyte/coating pair, but for the materials and chemicals reported on here, p/p_0 levels below 1–2% are appropriate. By understanding the limitations of molecular recognition materials in the context of gas and vapor sensing, designers of chemical sensor arrays can exploit these coatings to realize systems with significantly enhanced selectivity to a wide range of compounds.

ACKNOWLEDGMENT

The authors thank Prof. V. Schurig (Institute of Organic Chemistry, University of Tübingen) for providing the modified cyclodextrin and the nickel camphorate, and M. Hees and Prof. M. Hanack (Institute of Organic Chemistry, University of Tübingen) for providing the nickel phthalocyanine. Additionally, we thank C. Fietzek (Institute of Physical Chemistry, University of Tübingen) for determining some of the partition coefficients. We gratefully acknowledge the excellent technical assistance of A. W. Staton (Sandia National Laboratories) with SAW measurements and the measurement cell design and fabrication. We acknowledge many helpful technical discussions with Dr. Li Sun and Prof. R. M. Crooks (Department of Chemistry, Texas A&M University). Prof. Crooks also played a key role in conceiving our particular version of the combined SAW/FT-IR measurement system. Finally, we owe a debt of gratitude to Dr. Ross C. Thomas (Eltron, Inc.; formerly of Sandia National Laboratories), who led the design and setup of our SAW/FT-IR measurement system and demonstrated its viability. Sandia is a multiprogram laboratory operated by Sandia Corp., a Lockheed Martin Co., for the United States Department of Energy under Contract DE-AC04-94AL85000.

Received for review November 30, 1998. Accepted April 29, 1999.

AC981311J